nature geoscience

LETTERS

PUBLISHED ONLINE: 26 MAY 2013 | DOI: 10.1038/NGEO1827

Graphite formation by carbonate reduction during subduction

Matthieu E. Galvez[1,2]*†, Olivier Beyssac[1]*, Isabelle Martinez[2], Karim Benzerara[1], Carine Chaduteau[2], Benjamin Malvoisin[3,4] and Jacques Malavieille[5]

Carbon is transported from Earth's surface into its interior at subduction zones. Carbonates in sediments overlying hydrothermally altered rocks (including serpentinites) within the subducted slab are the main carriers of this carbon[1]. Part of the carbon is recycled back to the surface by volcanism, but some is transferred to the deep Earth[1,2]. Redox transformations during shallow subduction control the transfer and long-term fate of carbon, but are poorly explored[1,3]. Here we use carbon stable isotopes and Raman spectroscopy to analyse the reduction of carbonate in an exhumed serpentinite–sediment contact in Alpine Corsica, France. We find that highly crystalline graphite was formed during subduction metamorphism and was concentrated in the sediment, within a reaction zone in direct contact with the serpentinite. The graphite in this reaction zone has a carbon isotopic signature ($\delta^{13}C$) of up to 0.8 ± 0.1‰, similar to that of the original calcite that composed the sediments, and is texturally associated with the calcium-bearing mineral wollastonite that is also formed in the process. We use mass-balance calculations to show that about 9% of the total carbonaceous matter in the sedimentary unit results from complete calcite reduction in the reaction zone. We conclude that graphite formation, under reducing and low-temperature conditions, provides a mechanism to retain carbon in a subducting slab, aiding transport of carbon into the deeper Earth.

The transfer of carbon as carbonates between surface and deep reservoirs through subduction zones represents an overall annual flux of ~0.9–1.8 Tmol C yr^{-1} (refs 1,4). Several theoretical and experimental studies have shown that these carbonates might be destabilized by decarbonation[5] or dissolution[2,6] during metamorphism. Nonetheless, the respective contribution of these processes in releasing subducted C to exogenic reservoirs remains poorly assessed[4,7,8]. These destabilization processes are all strongly influenced by the composition and dynamics of metamorphic fluids[7,9]. For example, under oxidizing conditions carbonate destabilization may be associated with the loss of C in C-bearing fluid, mainly as CO_2. In contrast, reducing conditions modify the fate of carbonates during fluid–rock interactions[3]. Indeed, compelling field observations[10] and theoretical considerations[3] indicate that abiotic graphite can form under reducing conditions, but the importance of this process in subduction has not been assessed. In addition, owing to its lower solubility than carbonates under subduction conditions[2,3,6,11] and its lower mobility than carbonic fluids[10], graphite represents a highly refractory pool of C in subduction.

Here we report the massive transfer of C from carbonates to graphite that occurred at a metamorphosed serpentinite–sediment contact. This transfer is observed in a metamorphosed siliceous-carbonate unit outcropping along the Malaspina ridge in northern Alpine Corsica (Supplementary Fig. S1). The unit consists of blueschist metasedimentary rocks in direct contact with serpentinite. Peak metamorphic pressure–temperature (P–T) conditions, reached during the Alpine orogeny, are locally constrained to ~430 °C by geothermometry based on Raman spectroscopy of carbonaceous material (CM; see Methods) and ~9–15 kbar (refs 12,13). On the basis of tectono-stratigraphic arguments, this contact has been interpreted as a coherent segment of a former ocean–continent transition depositional setting[13,14] where reducing conditions might have been maintained throughout metamorphism[15]. The reaction zone (RZ) consists of a 5–10-cm-thick dark graphite-rich layer (see Supplementary Fig. S1). It occurs at the immediate interface between underlying serpentinite and metamorphic pristine sediment (PS) at its top. An 11-cm-long vertical section was cut through the serpentinite–sediment contact; it exhibits conspicuous mineralogical heterogeneities perpendicular to the contact (Fig. 1a). The upper part (PS) is pale grey to whitish with alternating layers of pelitic and quartz (Qtz)-rich lithologies (Fig. 1a). The pelitic horizons contain phengite (Phg) flakes and a low amount of graphitic CM; calcite (Cal) is widely present in the quartz-rich layers. A sharp transition is observed between the PS and the darker 4-cm-thick RZ (Fig. 1a and Supplementary Fig. S1). The RZ is composed of quartz, wollastonite (Wo, grey in Fig. 1a), Ca-rich garnet (Grt) and CM, and lacks calcite and phengite.

Sharp variations in the C content and C isotopic composition of the metasediments are observed across the RZ–PS transition (Fig. 1b–d and Supplementary Table S2). The total amount of CM (total organic carbon, TOC) increases by over an order of magnitude across the profile, ranging from 0.1 to 0.3 wt.% in the PS to 3–15 wt% in the RZ (Fig. 1b and Supplementary Table S2). The total C abundance (that is, inorganic (TIC) plus CM (TOC)) exhibits minor variations (Fig. 1b), except locally in a 5-mm-thick dark layer (Fig. 1a,b), showing the conservation of total C between the RZ and the PS. Values of $\delta^{13}C_{ORG}$ exhibit strong variations strictly matching the mineralogical zoning across the profile (Fig. 1a,c) increasing from $\delta^{13}C_{ORG} \sim -14$ to -12‰ in the PS to $+0.8$‰ in the RZ (Fig. 1c). The latter value is comparable to that of calcite in the PS and is among the heaviest C isotopic composition ever reported for any graphitic CM in metamorphic rocks, including fluid-deposited graphite[16]. Moreover, a slight

[1]IMPMC, CNRS-UPMC-IRD UMR 7590, UPMC Campus Jussieu, Case Courrier 115, 4 Place Jussieu, 75005 Paris, France, [2]Géochimie des Isotopes Stables, IPGP, PRES Sorbonne Paris Cité, 1 Rue Jussieu, 75005 Paris, France, [3]Laboratoire de Géologie, Département des Géosciences, ENS-CNRS, 24 Rue Lhomond, 75005 Paris, France, [4]ISTerre, CNRS UMR 5275, Université Grenoble I, BP 53 38041 Grenoble CEDEX 9, France, [5]Géosciences Montpellier, UMR 5243, CNRS-Université Montpellier II, 34095 Montpellier CEDEX 05, France. †Present address: Carnegie Institution of Washington, Geophysical Laboratory, 5251 Broad Branch Road NW, 20015 Washington DC, USA. *e-mail: matthieu.galvez@gmail.com; Olivier.Beyssac@upmc.fr

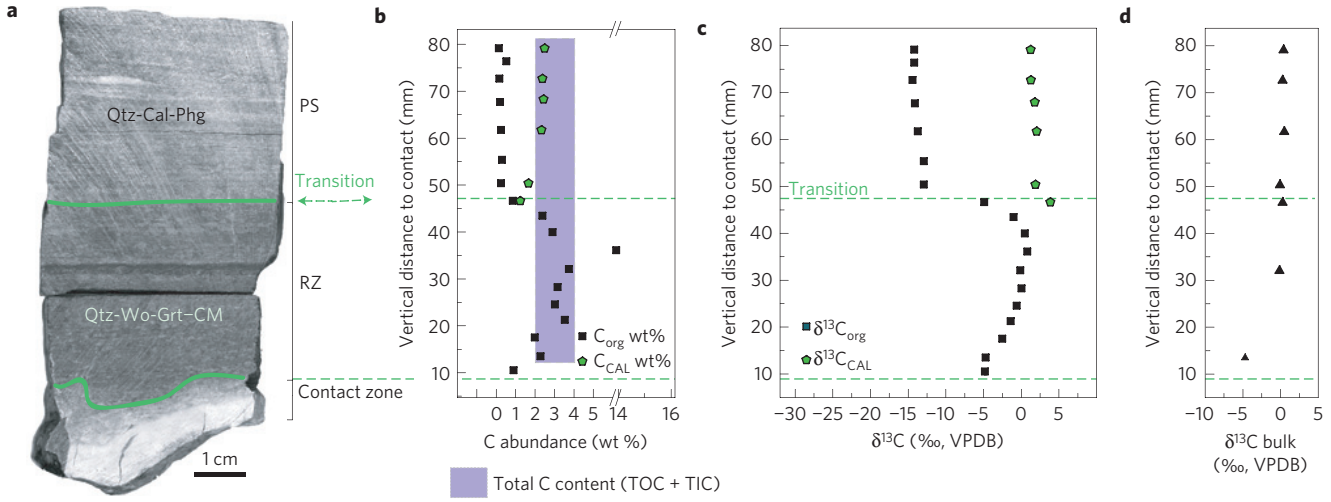

Figure 1 | Evolution of the C content and isotopic composition in the PS and the RZ. a, Photomicrograph of the rock chip corresponding to a section from the serpentinite contact zone to the unreacted PS. In **b**–**d** all geochemical data are represented versus the distance (in millimetres) to the contact with the serpentinite. **b**, Evolution of calcite (inorganic C, TIC) and CM content (TOC) along the profile and range of total C (TOC+TIC) content (purple area) in the rock. **c**, Evolution of the C isotopic composition along the profile. Error bars are smaller than the size of the symbol. **d**, Evolution of the bulk isotopic composition of **c**.

increase of $\delta^{13}C_{CAL}$ from +1.2‰ to +3.9‰ occurs within the PS downwards close to the transition with the RZ (Fig. 1C). In contrast to these variations, the bulk isotopic composition of C (weighted by the respective amounts of TOC and TIC) is conserved across the transition between the PS and the RZ (Fig. 1d). The conservation of total C abundance along with the anti-correlation between TOC and TIC evolution, as well as the similarity of $\delta^{13}C_{ORG}$ in the RZ with $\delta^{13}C_{CAL}$ in the PS, points to carbonate reduction as the main carbon source for the graphitic CM detected in the RZ. Moreover, the formation of this graphitic CM occurred under closed-system conditions with respect to C. Second-order TOC variations along the profile, especially in the 5-mm-thick dark layer within the RZ, can be ascribed to lithological variations (Fig. 1b) and/or local C redistribution.

Interestingly, the disappearance of calcite and increase in TOC perfectly match the appearance of wollastonite and correlate with important textural variations. In the PS, quartz and calcite are the main mineral phases (Fig. 2). Quartz is generally fine-grained and calcite occurs mostly as cement in the matrix (Fig. 2a). Conversely, the RZ is composed of a quartz matrix, foliated garnets and anhedral wollastonite grains that contain micrometric quartz and/or garnet inclusions (Fig. 2c,e). The garnet habit is highly similar to that of phengitic micas observed in the PS but absent from the RZ.

Besides, CM is a minor phase in the PS, occurring either as small disseminated grains or as flaky aggregates (Fig. 2a,b). On the contrary, CM is widespread in the RZ, appearing as coarse flaky grains in the quartz matrix (Fig. 2e), or forming continuous aggregates within the schistosity (Fig. 2f). Finally, CM also appears in the RZ as patches in close textural association with wollastonite and garnet (Fig. 2c,d), strongly supporting a co-genetic origin. The structural ordering of this abiotic CM in the RZ is markedly different from that of sedimentary CM contained in the PS as revealed by Raman microspectroscopy (Fig. 2g and Supplementary Fig. S3). Raman spectra obtained in the RZ and the PS are all characteristic of graphitic CM. However, the spectra from the PS exhibit intense defect bands, whereas these bands are significantly weaker in the RZ: this indicates that the crystallinity of graphitic CM is much higher in the RZ. Furthermore, in the second-order spectral region, the 2,700 cm^{-1} band is asymmetric in the RZ (see Supplementary Fig. S3), which indicates that this graphitic CM has reached the three-dimensional crystalline ordering of graphite[17]. This is not observed in the PS, where this band is symmetric, which shows that graphitic CM is turbostratic[17]. The structural heterogeneity (measured as variations among Raman spectra from different CM particles) is low within both the RZ and the PS, whereas variability is more pronounced close to the transition between the RZ and the PS with spectra ranging between the RZ and PS endmembers (Fig. 2g and Supplementary Fig. S3).

Together, these textural, isotopic and spectroscopic data strongly support the scenario in which carbonates are the source of abiotic graphite observed in the RZ according to the following reaction:

$$CaCO_3\,(Cal) + SiO_2\,(Qtz) \rightarrow CaSiO_3\,(Wo) + C\,(graphite) + 2O\,(fluid) \quad (1)$$

The exact speciation of the C–O–H fluid phase (represented by 2O here) is dependent on the P–T conditions and redox state of the system (see ref. 3, Methods and Supplementary Fig. S5).

Although it does not affect the significance of the reported carbonate reduction process, one can discuss whether calcite destabilization occurred during seafloor hydrothermalism before subduction, when Ca-rich (hydro)silicates can form[18] or, alternatively, during metamorphism in subduction. Seafloor serpentinization is widely regarded as favouring the abiotic synthesis of short-length hydrocarbons[19], which could serve as precursors to graphitic CM on incipient metamorphism. However, sedimentary CM in the PS and graphite in the RZ show very different degrees of graphitization. On the basis of existing field[20] and experimental studies[21], such a difference is better explained by formation of graphite in the RZ by abiotic nucleation and growth from a C-saturated COH fluid at a $T \sim 430\,^{\circ}C$ rather than through solid-state transformation (graphitization) of two different CM precursors at the same temperature. In addition, the presence of fibrous inclusions of aragonite in garnets present in the RZ (ref. 12) implies that garnet, and thus the RZ, must have formed under high P and low T metamorphic conditions, that is, within the stability field of aragonite (see Methods, Supplementary Figs S4 and S5). Therefore, the formation of the RZ during subduction is strongly supported by textural and petrological evidence, although its formation at lower pressure–temperature conditions during seafloor hydrothermalism cannot be completely ruled out at this stage. Thermodynamic calculations show that under equilibrium with a COH fluid, reaction equation (1) would

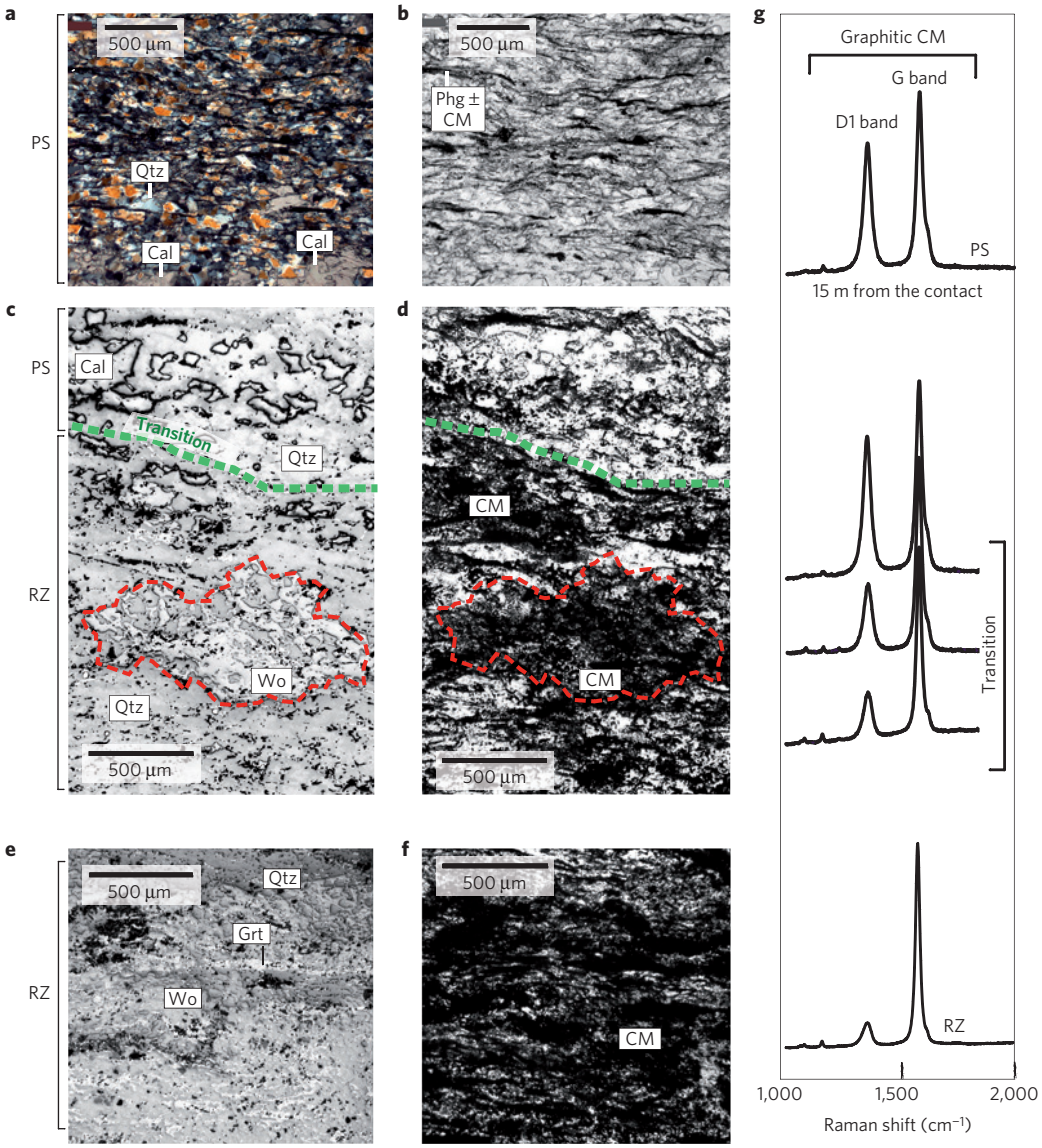

Figure 2 | Photomicrographs of representative mineralogical assemblages and graphitic textures in the sediment and reaction zone. a,**b**, Crossed-polar (**a**) and transmitted light (**b**) images of PS with quartz grains in a calcite matrix containing finely dispersed CM and coarse CM grains in phengite rich layers. **c**–**f**, The mineralogical contrast between the PS and the RZ is observed in reflected (**c**,**e**) and transmitted (**d**,**f**) light (the green dotted line underlines the PS–RZ transition). The textural association between CM (black) and wollastonite (or garnet; **e**,**f**) in the RZ is evidenced. The red dashed lines outline wollastonite (**c**) and CM (**d**). **g**, Representative Raman spectra showing the presence of turbostratic graphitic material within the PS and the high crystallinity of graphite within the RZ. This is shown by the variations of the relative area of the main defect band (D1 band) compared with the G band for graphitic C (see also Methods and Supplementary Fig. S2).

occur close to maximum water activity (Supplementary Fig. S5) involving a carbon-poor and slightly reducing fluid[3].

Our study reports the lowest temperature conditions (that is, 430 °C, Supplementary Fig. S4) for graphite formation in metamorphic rocks ever reported[22]. It also reveals that local chemical and redox heterogeneities created between contrasted lithologies (see also refs 9,23), such as between serpentinite and siliceous carbonate in widespread ocean–continent transition depositional settings of passive margins or mélanges zones[14,24], might ultimately control the fate of C in subduction. A better understanding of the redox effect of modern and exhumed lithological contacts might open new avenues to investigate the long-term fate of C in subduction zones.

Importantly, the destabilization of carbonates adjacent to the serpentinite at Malaspina was not followed by CO_2 devolatilization[7,25], but, instead, C was stored as graphite, which is chemically stable during high-pressure/low-temperature metamorphism. Thus, the formation of reduced C by abiotic processes can take place during shallow subduction provided reducing conditions are achieved. In addition, mass-balance calculations at the outcrop scale (see Methods) show that the amount of abiotic graphite formed by carbonate reduction in the RZ represents about 9% of the total CM (sedimentary CM + abiotic graphite) dispersed within the whole pile of the original sediment. This value is a first-order conservative estimate.

At the scale of a subduction zone (Fig. 3), the total carbonate input at the trench includes the flux of sedimentary carbonates (~0.9 (ref. 1) to ~1.8 (ref. 4) Tmol C yr^{-1}), as well as carbonates locked within the oceanic lithosphere, mainly in the upper oceanic crust (~2 ± 1 Tmol C yr^{-1} refs 1,4,26) and in serpentinites (~0.6 ± 0.2; ref. 27 to over 3.0 Tmol C yr^{-1}; ref. 4— Fig. 3). Processes such as dissolution and reduction of carbonates at depth are the least constrained factors[1] in present C cycling models, despite their

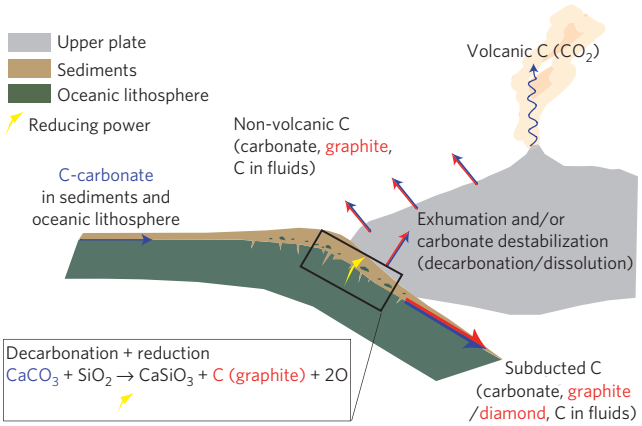

Figure 3 | Sketch illustrating the fate of carbonates in subduction zones including the carbonate reduction process triggering graphite formation. It highlights C transferred to the mantle as carbonates (blue arrow) or graphite (red arrow), as well as returning fluxes to the exogenic reservoirs through either volcanism, exhumation (non-volcanic C) or carbonate destabilization into fluid species (volcanic C). The figure is not to scale.

critical importance in controlling the long-term fate of C (Fig. 3). In strong support to this, we show that inventories of the mass and isotopic compositions of carbonate and reduced C reservoirs may be modified at shallow depth by carbonate reduction. Thus, carbonate destabilization in subduction zones does not necessarily imply C loss from the slab, either included within volcanic or non-volcanic C fluxes (Fig. 3). In contrast, under reducing and low fluid flux conditions, C might be locked as graphite in the slab and be either exhumed, or, alternatively, injected into the mantle, possibly acting as a precursor to other high-pressure C polymorphs (diamond; Fig. 3). Carbonate reduction to highly refractory graphitic CM might exert an overlooked control on C transfer between the Earth's surface and the deep Earth. Further work is needed to globally quantify the importance of this process.

Methods

Samples. Large polished petrological thin sections (10.5 cm) of the sample depicted in Fig. 1 were prepared for petrological observations using an OLYMPUS BX-51 microscope at the IPGP (Institut de Physique du Globe de Paris), and Raman analyses. Small chips were sampled from the rock section using a MECATOM T180 to perform isotopic analyses along a vertical profile. Further samples were collected across the outcrop far from the contact.

Stable isotopes. Aliquots of dried, carbonate-free (HCl (6 M) attack at 25 °C for 1 h and then 80 °C for 2 h) samples were added to cleaned quartz tubes and sealed under vacuum for combustion and oxidation with CuO (950 °C, 6 h) for CM extraction. CuO was first degassed for 1 h along with the storage quartz tubes at 900 °C; powder samples were then added before sealing under vacuum the pretreated tubes. For carbonates, the samples were attacked with H_3PO_4 at 25 °C for 4 h in a quartz tube before extraction in a vacuum line. After combustion, the tubes were slowly cooled to ambient temperature and opened on a vacuum line with a tube cracker. The CO_2 was separated cryogenically from the combustion gases using a liquid nitrogen trap, and quantified with a manometer. The C isotope compositions of the purified CO_2 gas were measured using a Finnigan delta + XP mass spectrometer at IPGP working in dual inlet mode. The internal precision of the isotopic measurements is 0.05‰. All results are reported in Supplementary Table S3 using the conventional δ notation versus PDB (Pee Dee Belemnite) standard for C isotopes: $\delta^{13}C = [(^{13}C/^{12}C)_{smp}/(^{13}C/^{12}C)_{std} - 1] * 1{,}000$, where smp refers to the sample and std to the standard (PDB in the case of $\delta^{13}C$).

Sensitivity analysis. The procedure used to compute the uncertainty induced by the extraction procedure on isotopic measurements of CM takes into account the chain of steps that propagates uncertainties for the TOC and $\delta^{13}C$ measurements during the analytical process. We used a Monte Carlo analysis that gathers 2,000 trials to evaluate the analytical uncertainty for each of the extraction steps. We performed a test on a C-free material (pure quartz) to measure the amount of C added to the samples due to the extraction procedure and sample handling. From all of these analyses, we estimate that when the quantity of sample introduced within the sealed tube exceeds 200 mg, 2.5 µmol of contaminating CO_2 with $\delta^{13}C_{BLANK} = -25 \pm 2$‰ is added to our measurements. For quantities lower than 200 mg, we assume from these tests that 1.5 µmol of contaminating CO_2 with a similar isotopic composition ($\delta^{13}C_{BLANK} = -25 \pm 2$‰) is added. For each sample, the standard deviations provided by Monte Carlo analyses (0.1–0.4 ‰) were taken as the uncertainty for each individual measurement (Supplementary Table S3).

Raman microspectroscopy. Raman spectra were measured using a Renishaw InVIA Reflex microspectrometer equipped with a 514 nm LaserPhysics (20 mW) argon laser at the Institut de Mineralogie et de Physique des Milieu Condenses (IMPMC). Before each session, the spectrometer was calibrated with a silicon standard. The laser was focused on the sample by a DMLM Leica microscope with a ×100 objective (numerical aperture = 0.85), and the laser power at the sample surface was set at around 1 mW to avoid damage due to laser-induced heating. The signal was filtered by edge filters and finally dispersed using a 1,800 gr mm^{-1} grating to be analysed by a Peltier cooled RENCAM CCD (charge-coupled device) detector. Before each session, the spectrometer was calibrated with a silicon standard. As Raman analysis of CM may be affected by several analytical mismatches, we strictly followed the analytical procedure described in ref. 17. For thermometry based on Raman spectroscopy of CM, more than 30 spectra were recorded on PS samples collected far from the contact, in which CM derives from graphitization of sedimentary CM during metamorphism, and is not abiotic graphite (Supplementary Figs S2 and S4).

We used the extended scanning mode to record large spectral windows from 1,000 to 2,000 cm^{-1}; this spectral range is necessary to clearly measure the whole background signal and to properly define the baseline. Spectra were fitted using the Peakfit software.

Mass-balance estimation. The estimation of the fraction of abiotic graphite (F) in a vertical column (1 m^2) of the outcrop was bracketed considering a mean sedimentary CM content in the 15-m-thick PS, ($[CM]_{PS}$) of 0.1 wt%, whereas we considered a mean CM content of 3 wt% in a 5-cm-thick RZ ($[CM]_{RZ}$), following:

$$F = 0.05 * [CM]_{RZ} / (15 * [CM]_{PS} + 0.05 * [CM]_{RZ})$$

Received 31 October 2012; accepted 17 April 2013; published online 26 May 2013

References

1. Hayes, J. M. & Waldbauer, J. R. The carbon cycle and associated redox processes through time. *Phil. Trans. R. Soc. Lond. B* **361,** 931–950 (2006).
2. Frezzotti, M. L., Selverstone, J., Sharp, Z. D. & Compagnoni, R. Carbonate dissolution during subduction revealed by diamond-bearing rocks from the Alps. *Nature Geosci.* **4,** 703–706 (2011).
3. Connolly, J. Phase diagram methods for graphitic rocks and application to the system C–O–H–FeO–TiO_2–SiO_2. *Contrib. Mineral. Petrol.* **119,** 94–116 (1995).
4. Evans, K. A. The redox budget of subduction zones. *Earth Sci. Rev.* **113,** 11–32 (2013).
5. Greenwood, H. Wollastonite: Stability in H_2O–CO_2 mixtures and occurrence in a contact-metamorphic aureole near Salmo, British-Columbia, Canada. *Am. Mineral.* **52,** 1669–1680 (1967).
6. Caciagli, N. C. & Manning, C. E. The solubility of calcite in water at 6–16 kbar and 500–800°C. *Contrib. Mineral. Petrol.* **146,** 275–285 (2003).
7. Gorman, P. J., Kerrick, D. M. & Connolly, J. A. D. Modeling open system metamorphic decarbonation of subducting slabs. *Geochem. Geophys. Geosyst.* **7,** Q04007 (2006).
8. Evans, K. Metamorphic carbon fluxes: How much and how fast? *Geology* **39,** 95–96 (2011).
9. Ague, J. J. Release of CO_2 from carbonate rocks during regional metamorphism of lithologically heterogeneous crust. *Geology* **28,** 1123–1126 (2000).
10. Evans, K. A., Bickle, M. J., Skelton, A. D. L., Hall, M. & Chapman, H. Reductive deposition of graphite at lithological margins in East Central Vermont: S Sr, C and O isotope study. *J. Metamorph. Geol.* **20,** 781–798 (2002).
11. Frost, B. R. Mineral equilibria involving mixed-volatiles in a C–O–H fluid phase; the stabilities of graphite and siderite. *Am. J. Sci.* **279,** 1033–1059 (1979).
12. Chopin, C., Beyssac, O., Bernard, S. & Malavieille, J. Aragonite-grossular intergrowths in eclogite-facies marble, Alpine Corsica. *Eur. J. Mineral.* **20,** 857–865 (2008).
13. Vitale Brovarone, A. *et al.* Stacking of continuous segments of subducted lithosphere in high-pressure orogens: architecture of Alpine Corsica (France). *Earth Sci. Rev.* **116,** 35–56 (2013).
14. Manatschal, G. & Muntener, O. A type sequence across an ancient magma-poor ocean–continent transition: The example of the western Alpine Tethys ophiolites. *Tectonophysics* **473,** 4–19 (2009).
15. Malvoisin, B., Chopin, C., Brunet, F. & Galvez, M. E. Low-temperature wollastonite formed by carbonate reduction: A marker of serpentinite redox conditions. *J. Petrol.* **53,** 159–176 (2012).

16. Luque, F. J., Crespo-Feo, E., Barrenechea, J. F. & Ortega, L. Carbon isotopes of graphite: Implications on fluid history. *Geosci. Front.* **3,** 197–207 (2012).
17. Beyssac, O. *et al.* On the characterization of disordered and heterogeneous carbonaceous materials by Raman spectroscopy. *Spectrochim. Acta A* **59,** 2267–2276 (2003).
18. Frost, B. R., Beard, J. S., McCaig, A. & Condliffe, E. The formation of micro-rodingites from IODP hole U1309D: Key to understanding the process of serpentinization. *J. Pet.* **49,** 1579–1588 (2008).
19. McCollom, T. M. & Seewald, J. S. Abiotic synthesis of organic compounds in deep-sea hydrothermal environments. *Chem. Rev.* **107,** 382–401 (2007).
20. Beyssac, O., Goffé, B., Chopin, C. & Rouzaud, J-N. Raman spectra of carbonaceous material in metasediments: A new geothermometer. *J. Metamorph. Geol.* **20,** 859–871 (2002).
21. Beyssac, O., Brunet, F., Petitet, J.-P., Goffé, B. & Rouzaud, J.-N. Experimental study of the microtextural and structural transformations of carbonaceous materials under pressure and temperature. *Eur. J. Mineral.* **15,** 937–951 (2003).
22. Luque, F. J., Pasteris, J. D., Wopenka, B., Rodas, M. & Barrenechea, J. F. Natural fluid-deposited graphite; mineralogical characteristics and mechanisms of formation. *Am. J. Sci.* **298,** 471–498 (1998).
23. Miyashiro, A. Oxidation and reduction in the Earth's crust with special reference to the role of graphite. *Geochim. Cosmochim. Acta* **28,** 717–729 (1964).
24. Marschall, H. R. & Schumacher, J. C. Arc magmas sourced from melange diapirs in subduction zones. *Nature Geosci.* **5,** 862–867 (2012).
25. Kerrick, D. M. & Connolly, J. A. D. Metamorphic devolatilization of subducted marine sediments and the transport of volatiles into the Earth's mantle. *Nature* **411,** 293–296 (2001).
26. Alt, J. C. & Teagle, D. A. H. The uptake of carbon during alteration of ocean crust. *Geochim. Cosmochim. Acta* **63,** 1527–1535 (1999).
27. Alt, J. C. *et al.* Recycling of water, carbon, and sulfur during subduction of serpentinites: A stable isotope study of Cerro del Almirez, Spain. *Earth Planet. Sci. Lett.* **327-328,** 50–60 (2012).

Acknowledgements

This project was financially supported by the ANR JC programme (project GeoCarbons, PI O. Beyssac), CNRS-INSU and the Ville de Paris Emergence programme (project Cycle géologique du carbone organique, PI O. Beyssac). Particularly insightful reviews by D. Rumble and J. Connolly of early versions of the manuscript were much appreciated. This work also benefited from various discussions with C. Chopin, P. Agrinier, J. Dubessy, P. Cartigny, V. Busigny, A. Vitale Brovarone, M. Clog, P. Sans-Jofre, G. Cody and O. Vidal. Finally, we thank J. J. Bourrand and M. Ader for technical assistance.

Author contributions

M.E.G., O.B., I.M. and K.B designed the research and performed field work, analysed data and wrote the paper; M.E.G performed laboratory work; C.C. developed analytical tools, analysed data and wrote the paper; B.M. and J.M. performed field work, analysed data and wrote the paper.

Additional information

Supplementary information is available in the online version of the paper. Reprints and permissions information is available online at www.nature.com/reprints. Correspondence and requests for materials should be addressed to M.E.G. or O.B.

Competing financial interests

The authors declare no competing financial interests.